An Imaging System Exhibiting Wavelength-Dependent Resolution

By S. Y. CHAI

(Manuscript received January 20, 1969)

The Christiansen filter consists of particles of a transparent solid immersed in a suitable liquid such that the two materials have different dispersions but equal indexes of refraction at some specified wavelength. This paper analyzes such a filter as an optical device for providing wavelength-dependent resolution.

We derive the modulation transfer function of this filter by using the Huygens–Fresnel diffraction principle. General agreement is obtained with experimental measurements made using monochromatic light.

One proposed single-tube color camera system for picture telephone service requires the three primary color component images to have different resolutions. An optical filter illustrating the characteristics required by this application was designed using the formulas developed in this paper. Subjective evaluation of the experimental results obtained with this filter indicates no unforeseen degradation of the composite image of the primary color components.

I. INTRODUCTION

When homogeneous isotropic particles, such as crushed optical glass, are immersed in a liquid which has, at a specified wavelength, the same index of refraction as the particles but a different dispersion, light at the specified wavelength is unaffected in passing through the mixture. On the other hand, light of other wavelengths is dispersed. A cell containing such a mixture of solid particles in an appropriate liquid constitutes a Christiansen filter (see Figure 1).[1–4]

The wavelength dependent action of the filter can be used to construct a low-pass spatial filter with a wavelength dependent cut-off. In particular, with the proper glass particles and liquid, the filter acts as weakly diffusing ground glass for the blue and red images while not affecting the green images.

An optical device using a color-selective spatial low-pass filter of this type is desirable in order to realize a proposed single pickup-tube color camera.[5,6] In this camera, color separation is achieved by modulating the amplitude of the color signals onto different carrier frequencies. These carrier frequencies are in turn generated by striped filters that have different spatial frequencies for the different primary colors. It is necessary to reduce the spatial bandwidth of the composite color image in order to meet the resolution limitation of the camera tube.

This bandwidth reduction can be used because the human eye does not readily discriminate between composite images composed of three high resolution primary color images, and a composite image composed of a high resolution green image and low resolution red and blue images.

By considering the filter as a random phase-changing screen, one can determine its spatial frequency response as a function of glass particle size, thickness of the filter, and position of the filter in relation to the image plane.[4,7]

The quantitative understanding thus gained is used to design an optical filter with characteristics which are roughly those which would be required by an experimental color picture telephone system. The experimentally observed effect of this filter indicated no unforeseen degradation of the subjective quality of the final composite image transmitted through it.

II. OPTICAL TRANSFER FUNCTION OF THE FILTER SYSTEM

Figure 1 shows an optical system transforming an object plane into an image plane. If the object plane is incoherently illuminated, the system is linear in intensity and therefore:

$$i(x, y) = \iint o(x', y')h(x - x', y - y')\,dx'\,dy' \tag{1}$$

where $i(x, y)$ and $o(x', y')$ are the intensity distribution in the image plane and object plane, respectively; and the point spread function h of the optical system represents the intensity distribution in the image plane for a point object.

In terms of spatial frequency (f_x, f_y) response, we have

$$I(f_x, f_y) = O(f_x, f_y)H(f_x, f_y) \tag{2}$$

where the optical transfer function $H(f_x, f_y)$ is the Fourier transform

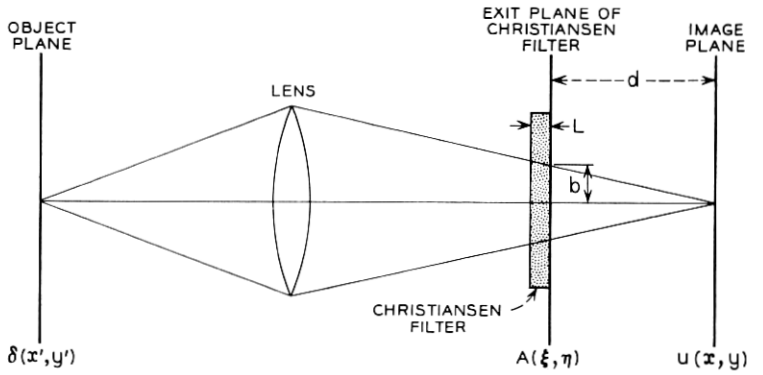

Fig. 1 — Optical system with Christiansen filter.

of the point spread function h. If the transfer function is real and only the modulus is used, it is then called the modulation transfer function.[8]

The point spread function h, by definition, is:

$$h(x, y) = u(x, y) \cdot u(x, y)^* \tag{3}$$

where $u(x, y)$ is the complex amplitude distribution of a point object in the image plane. This is called the "point image function," and $u(x, y)^*$ is its complex conjugate.

Using the Huygens-Fresnel diffraction principle, the point image function $u(x, y)$ can be expressed in terms of the complex field distribution $A(\xi, \eta)$ over the exit plane of the filter (see Fig. 1).[9-11] We should pay particular attention to the fact that we are assuming a point object and an isoplanatic region. That is, the optical system is assumed linear such that equation (1) holds throughout the entire object plane. Thus, for a point object, the point image function is given by

$$u(x, y) = \frac{1}{j\lambda} \frac{e^{jkd}}{d} \iint_{-\infty}^{+\infty} A(\xi, \eta) \exp\left\{\frac{jk}{2d}[(\xi - x)^2 + (\eta - y)^2]\right\} d\xi\, d\eta. \tag{4}$$

The field distribution in the exit plane of a thin Christiansen filter can be written as

$$A(\xi, \eta) = E_o(\xi, \eta) e^{i\Phi(\xi, \eta)} \cdot \exp\left[-\frac{jk}{2d}(\xi^2 + \eta^2)\right] \tag{5}$$

where $\Phi(\xi, \eta)$ is a random phase function produced by scattering (see

the appendix), and the term $E_o(\xi, \eta) \exp[-jk/2d\ (\xi^2 + \eta^2)]$ represents the spherical wavefront produced by the lens. Since the field outside the lens aperture is suppressed,

$$E_o(\xi, \eta) = \begin{cases} \text{constant} & (\xi^2 + \eta^2)^{\frac{1}{2}} \leqq b \\ 0, & (\xi^2 + \eta^2)^{\frac{1}{2}} > b \end{cases}$$

and b is proportional to the lens aperture as shown in Fig. 1.

Since the phase function $\Phi(\xi, \eta)$ was assumed to be a two-dimensional random process with isotropic fluctuation, and the experimental test object contains only one-dimensional variations in the transmission, the problem can be reduced to one dimension for simplicity. Thus, by neglecting the constant factor outside the integrals, we may rewrite equation (4) as

$$\begin{aligned} u(x) &= \int_{-\infty}^{+\infty} E_o(\xi) e^{j\Phi(\xi)} \exp\left(-\frac{jk}{2d}\xi^2\right) \cdot \exp\left\{\frac{jk}{2d}(\xi - x)^2\right\} d\xi \\ &= \exp\left(\frac{jk}{2d}x^2\right) \int_{-\infty}^{+\infty} E_o(\xi) e^{j\Phi(\xi)} \exp\left(-\frac{jk}{d}\xi x\right) d\xi. \end{aligned} \tag{6}$$

The optical transfer function $H(f_x)$ of the system is now obtained by taking the Fourier transformation of $u(x)u(x)^*$ to give

$$\begin{aligned} H(f_x) &= \int_{-\infty}^{+\infty} u(x)u(x)^* \exp(j2\pi f_x x)\, dx \\ &= \int_{-\infty}^{+\infty} E_o(\xi) e^{j\Phi(\xi)} \cdot \{E_o(\xi - d\lambda f_x) \exp[j\Phi(\xi - d\lambda f_x)]\}^*\, d\xi. \end{aligned} \tag{7}$$

Normalizing (dropping the subscript x) this equation results in

$$H(f) = \frac{\displaystyle\int_{-\infty}^{+\infty} E_o(\xi) e^{j\Phi(\xi)} \{E_o(\xi - d\lambda f) \exp[j\Phi(\xi - d\lambda f)]\}^*\, d\xi}{\displaystyle\int_{-\infty}^{\infty} |\, E_o(\xi)\,|^2\, d\xi}. \tag{8}$$

The statistics of the phase fluctuation $\Phi(\xi)$ are assumed to be such that the average value with respect to ξ can be replaced by an ensemble average. By denoting an ensemble average by $\langle\ \rangle_{av}$, the normalized transfer function for this case becomes

$$H(f) = D(f)\langle \exp\{j[\Phi(\xi) - \Phi(\xi - d\lambda f)]\}\rangle_{av} \tag{9}$$

where

$$D(f) = 1 - \frac{d\lambda f}{2b} \cong 1.$$

Because the range of the spatial frequency f under discussion is much lower than the cutoff frequency produced by diffraction at the lens aperture, $d\lambda f$ is much less than $2b$. Therefore, $D(f)$ can be approximated by unity.

Under the condition that $\Phi(\xi)$ is a random gaussian variable of zero mean and variance Φ_o^2, equation (9) is shown to be[12]

$$H(f) = \exp \{-\Phi_o^2[1 - \rho(d\lambda f)]\} \tag{10}$$

where $\rho(d\lambda f)$ is the autocorrelation function for the phase fluctuations at the exit plane of the filter and is expressed as

$$\rho(d\lambda f) = \frac{\int \Phi(\xi)\Phi(\xi - d\lambda f)\, d\xi}{\int \Phi(\xi)^2\, d\xi}. \tag{11}$$

Now, the autocorrelation function $\rho(d\lambda f)$ must be determined. The behavior of the function ρ is complicated; however, it is known that

$$\rho(d\lambda f) = 1 \quad \text{when} \quad d\lambda f = 0$$

and

$$\rho(d\lambda f) = 0 \quad \text{when} \quad d\lambda f \text{ is greater than the linear dimension of the scattering particles.}$$

In this case there are many possible types of behavior that the function $\rho(r)$ may exhibit. Two common types are.[13–16]

$$\rho(r) = \exp(-|r/q|) \tag{12a}$$

and

$$\rho(r) = \exp[-(r/q)^2] \tag{12b}$$

where the q represents a correlation length.
These are both particularly important forms to us because we are interested primarily in small r. Thus, equations (12a) and (12b) reduce to

$$\rho(r) \cong 1 - \left|\frac{r}{q}\right| \tag{13a}$$

and

$$\rho(r) \cong 1 - \frac{r^2}{q^2}. \tag{13b}$$

The autocorrelation function for any particles, regardless of shape, reduces to one of these two forms for small r. In our experiments we assumed spherical particles and equation (13a) is found to be the more realistic approximation. Thus, let us assume[15,16]

$$\rho(d\lambda f) = \exp\left\{ - \left| \frac{d\lambda f}{K2a} \right| \right\} \tag{14}$$

where the diameter $2a$ of the particle indicates the order of the size of the irregularities. The constant K is a factor expressing the actual correlation length to the diameter of the particle and can be obtained from the function $\rho(d\lambda f)$ which is empirically determined. Only the small values of $d\lambda f$ are of interest so that by approximating equation (14)

$$\rho(d\lambda f) \cong 1 - \left| \frac{d\lambda f}{K2a} \right|. \tag{15}$$

Finally, substituting equations (15) and (27) into equation (10), the modulation transfer function obtained is

$$H(f) = \exp\left\{ - \frac{3.29CL \, \triangle n^2 \, df}{K\lambda} \right\} \tag{16}$$

where C is the ratio of particle volume to total volume, L is the thickness of the filter, and $\triangle n$ is the difference in refractive index between particles and liquid.

Notice that when f is very large so that $\rho(d\lambda f) \cong 0$, the modulation transfer function reaches a constant value of

$$H(f) = \exp\{-\Phi_o^2\} = \exp\left\{ - \frac{6.58CLa \, \triangle n^2}{\lambda^2} \right\}. \tag{17}$$

This means that there is always finite transmission at high spatial frequencies, but that the loss can be made as large as desired by controlling the parameters of equation (17).

III. EXPERIMENTAL

3.1 *Preparation of Filters*

The filters were made of crown glass type K5 ($N_d = 1.52320$) in a solution of ethyl salicylate at room temperature. This combination provides a nearly transparent filter in the green region as shown in Fig. 2. The dispersion curves were determined by a Carl Zeiss, Model A Abbe-refractometer.

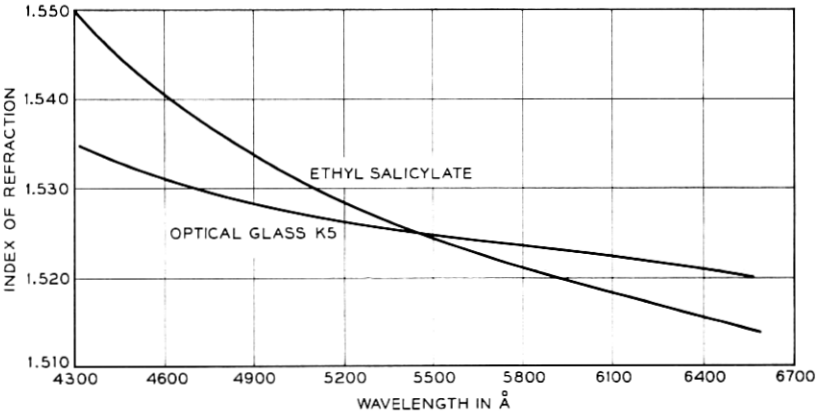

Fig. 2 — Dispersion curves of optical glass (*K5*) and ethyl salicylate.

The glass particles were prepared by pulverizing them with a ball mill; they were then cleaned with aqua regia and distilled water. The size of the particles was estimated by averaging the dimensions of the wire screen used in sorting. The radii of the prepared samples ranged from 37μ to 44μ, 44μ to 62μ, 75μ to 125μ, and 125μ to 150μ. The cells were made by epoxy-cementing glass plates to 1-inch diameter glass tubing of lengths 2mm, 2.5mm, 3.5mm, and 4mm.

The cells were about half filled with the liquid, then the glass particles were poured in slowly so that air bubbles were not carried down. The volume of the glass particles was determined from their weight and known density of 2.59 grams per cubic centimeter. The volume ratio C was found to be approximately 0.42, independent of particle size.

3.2 *Measurement of Modulation Transfer Function*

The apparatus used to measure the transfer function of the optical system has been described previously.[17] Figure 3 is a rough sketch of this apparatus. A target film with sinusoidal intensity distribution was used as a test object. The film was imaged through the Christiansen filter onto a slit in front of the photomultiplier. Rotation of the drum containing the test film caused the image to move across the sampling slit. The sinusoidal gratings of the test film varied logarithmically from 4 to 300 cycles per inch and were arranged on the target film in sequence to allow rapid measurement or direct recording of the modulation transfer function.

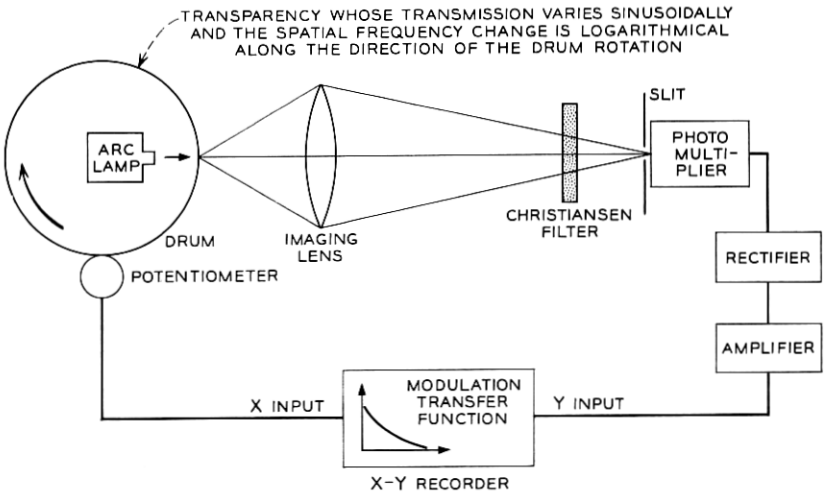

Fig. 3 — Apparatus for measuring the modulation transfer function of the filter.

The measurements were usually carried out in the region of the blue mercury arc light to maximize the response of the S-11 photomultipler. The slit width of the photomultiplier was 100μ, which corresponds to a sampling interval equal to one-third the period of highest frequency. An $f/2.3$ lens of 5-cm focal length was used to image the target film onto the slit. The target-lens spacing was 6 cm and the lens-slit spacing was 30 cm. This resulted in a magnification of 5 and gave a range of spatial frequencies from about 0.03 cycles per millimeter to 3 cycles per millimeter. This range of spatial frequencies is of interest for potential color picture telephone camera applications.

The target film was first focused with a cell filled with only the liquid placed between the lens and the slit. This compensates for the increased optical path length resulting from the nonunity index of refraction of the Christiansen filter.

IV. RESULTS AND DISCUSSION OF THE MODULATION TRANSFER FUNCTION

The modulation transfer functions of the filters were measured for various positions of the filters as well as for various thicknesses and particle sizes of the filter. The position of the filter was defined by the distance d between the slit plane and the inside of the exit glass plate of the cell (see Fig. 1).

The experimentally determined modulation transfer functions, for

several different filter positions with a filter thickness of 2.5 mm and particle radius of 100 μ, are plotted in Fig. 4. Figure 5 shows the variation of the modulation transfer functions with filter thickness for a constant particle radius of 100 μ and a d of 1/8-inch. From Fig. 4, the linear dependence of the exponent $\Phi_o^2(1 - \rho)$ on d can be demonstrated, thus validating equation (10). In addition, Fig. 5 shows the approximately linear dependence of Φ_o^2 on L, indicating the validity of equation (27). From these results, the assumption of equation (15) for the autocorrelation function of the phase irregularities also appears reasonable.

The dependence of the modulation transfer function on particle size is shown in Fig. 6. From this figure, the factor K representing the ratio of the particle diameter to correlation length [see equation (14)] was obtained and plotted in Fig. 7 as a function of the particle size a. A quantitative analysis of the effect of the particle size on the transfer function is unavailable because the exact expression for the phase autocorrelation function in terms of the particle size is not known. It is believed that the empirically determined factor K provides a qualitative dependence of the particle size on the phase autocorrelation function because only small values of $d\lambda f/2aK$ [see equation (14)] are of interest. A theoretical analysis of the phase autocorrelation function may not be of great value unless the exact shape of the particle is considered.

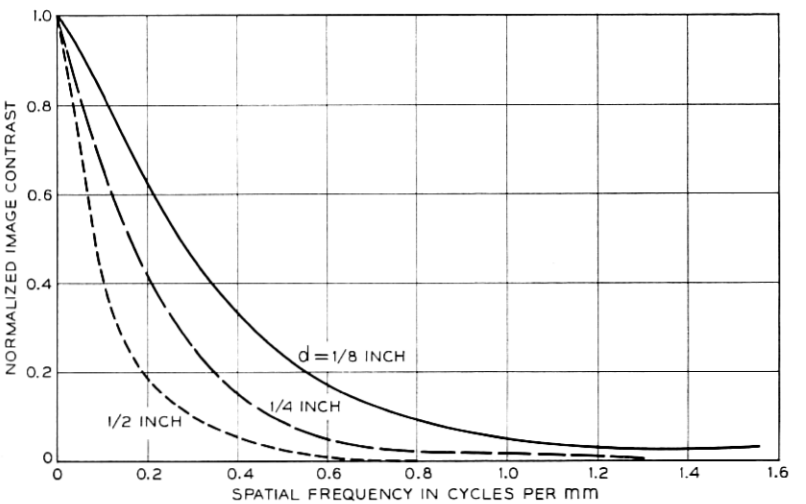

Fig. 4 — Experimental modulation transfer functions for various filter positions ($a = 100\mu$, $d = 2.5$ mm, $\lambda = 4358$ Å).

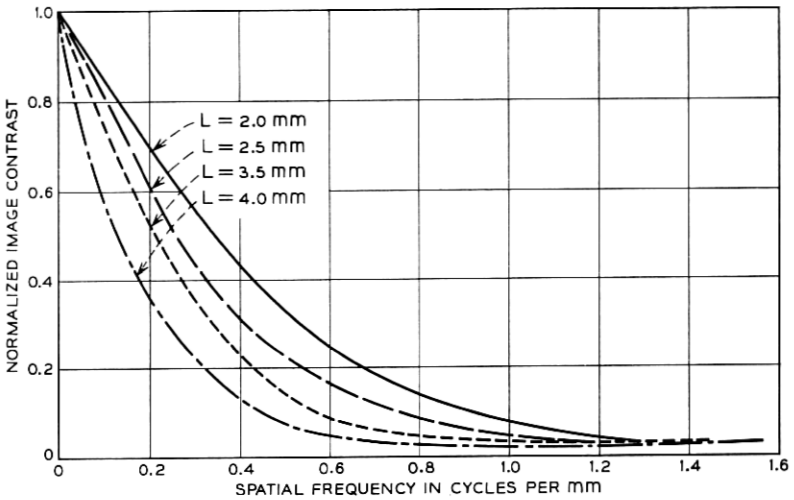

Fig. 5 — Experimental modulation transfer functions for various filter thickness ($a = 100\mu$, $d = 3.18$ mm, $\lambda = 4358$ Å).

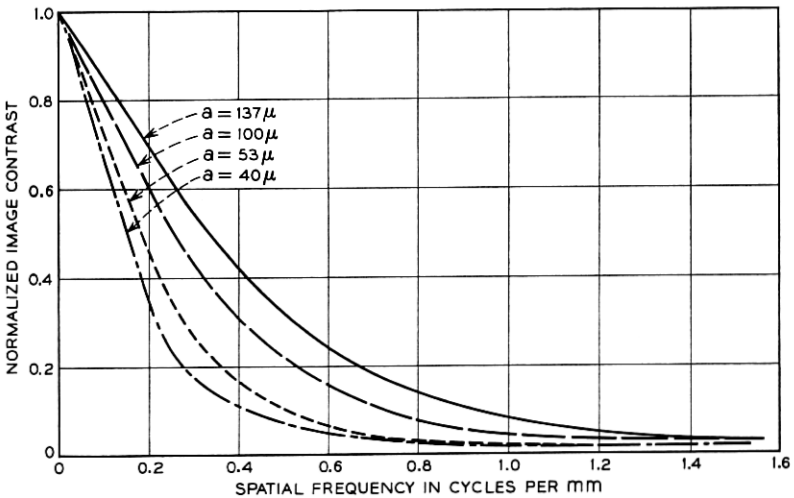

Fig. 6 — Experimental modulation transfer functions for various particle sizes of the filter ($L = 2.5$ mm, $d = 3.18$ mm, $\lambda = 4358$ Å).

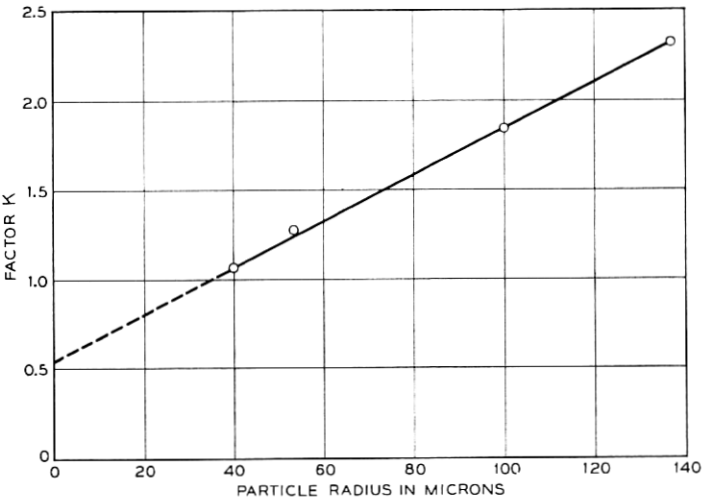

Fig. 7 — Factor K of phase correlation length versus particle sizes.

The linear dependence of the factor K on the particle size a, shown in Fig. 7, cannot be extended much further than the radius of about 150μ because the gaussian phase fluctuation imposes an upper limit on a for which the central limit theorem is applicable (see the appendix). In practice, it is not possible to determine the exact correlation length from Fig. 7, since it is impossible to obtain a large value of the correlation length $2aK$ with sufficient accuracy from extrapolation of the small values of $d\lambda f$.

In order to simulate a situation of independent resolution control of primary color images, measurements of the transfer functions at the blue, green, and red regions were made with a Christiansen filter 2.5mm thick and with a 100μ particle radius. In this case, the filter was set $\frac{1}{8}$-inch away from the image plane. As light sources of primary colors, a mercury arc lamp was filtered with Optics Technology, Inc., monopass filters, No. 433 for blue (4350 Å), No. 566 for green (5600 Å), and No. 633 for red (6250 Å).* Figure 8 shows the results. The modulation transfer function for the imaging lens itself also is plotted in Fig. 8 to show the effect of the lens aberrations.

* These narrow band filters were used in order to give quantitative agreement with theory. In its proposed application to resolution control the true "wide band" primaries should be used. The evaluation of this filter for resolution control in a TV color camera is more involved and is the subject of the following sections.

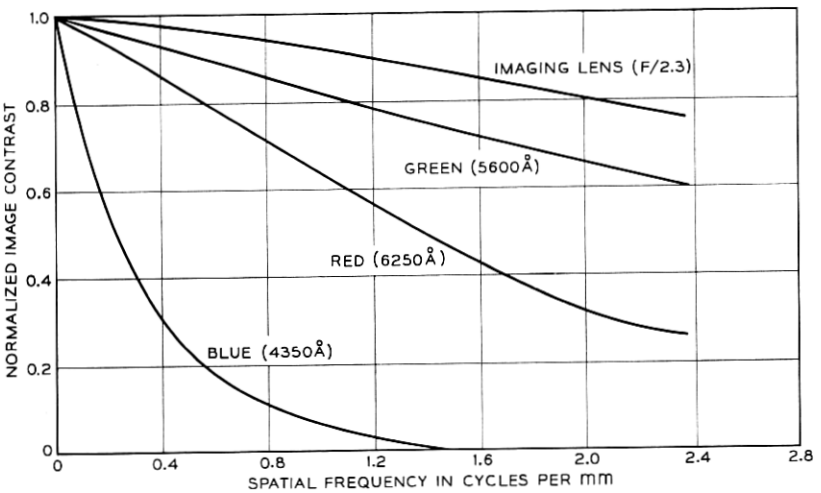

Fig. 8 — Experimental modulation transfer functions for different wavelengths and for imaging lens with $a = 100\mu$, $L = 2.5$ mm, and $d = 3.18$ mm.

Figure 9 shows the comparison between the experimental results at different wavelengths and the theoretical modulation transfer function given by equation (16). The values of Δn used in this equation, 1.5×10^{-2} at $\lambda = 4350$ Å, 10^{-3} at $\lambda = 5600$ Å and 6×10^{-3} at $\lambda = 6250$ Å, were obtained from Fig. 2. The factor K of 1.82 obtained from Fig. 7 and the measured value C of 0.42 are also used in equation (16). The experimental results are plotted from Fig. 8 after correcting for the effects of the aberrations caused by the imaging lens. This correction becomes necessary at the higher spatial frequencies encountered with red and green light.

The deviation between the experimental and analytical results probably result from thermally induced changes in the refractive index of ethyl salicylate, which has a thermal coefficient of index of refraction of about 5×10^{-4} per C°. A slight change in Δn causes a significant change in the analytical results for the green region, since Δn for green is a small value. On the other hand, the effect of a small change in Δn has very little effect on the calculated blue or red responses. Choosing the correct value of Δn to be used in equation (16) is further complicated by the 100 Å spectral bandwidth of the primary colors used.

The theoretical and experimental results shown in Fig. 9 agree sub-

stantially considering the many approximations made. These approximations include the representation of the actual particles by spheres with no variation in particle size and assuming a filter thin enough to allow the difference in path length through the filter between normally and obliquely incident rays to be neglected.

V. APPLICATION OF THE FILTER

As Section IV shows, the cutoff frequency of the modulation transfer function (spatial frequency response) of the Christiansen filter can be controlled by the filter thickness, the particle size, and the position of the filter with respect to the image plane. Using this quantitative understanding, a filter for independently controlling the resolutions of the three superposed primary color images was designed. The operation of the filter and its suitability for the intended application were then experimentally verified.

In order to evaluate the filter in its proposed application to the color picture telephone system, the true NTSC primary color "taking" filters were used.

5.1 *Evaluation of the Filter*

For the color camera, the desirability of having the shortest possible distance between the filter and the image plane (that is camera

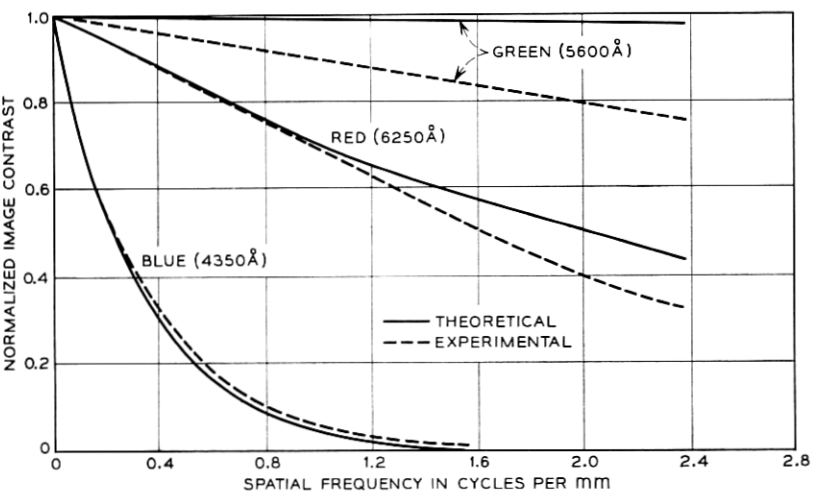

Fig. 9 — Comparison of experimental and theoretical modulation transfer functions for selected wavelengths with $a = 100\mu$, $L = 2.5$ mm, and $d = 3.18$ mm.

tube target) dictates choosing a glass particle with about a 40μ radius. The filter had a circular cross section 20 mm in diameter, and it was 2.5 mm thick.

The experimental arrangement used is shown in Fig. 10. Incandescent (white) light illuminated a ground glass diffuser which was positioned in front of the 35 mm color slide used to simulate a real object. In order to be able to separate the three primary color images, the incandescent (white) light was actually derived by adding the primary colors with the half-silvered mirrors as shown in Fig. 10. The primary colors were generated by projecting tungsten filament light through the appropriate Wratten filters: No. 25 for red, No. 47B for blue, and No. 58 for green.

A Bell and Howell $f/1.3$ Angeniux television camera lens with a 15 mm focal length was used as an object lens. The image size was about 10 mm by 10 mm to simulate the raster size of a typical picture telephone camera. For viewing, the image formed at the image plane (that is, vidicon tube target) was magnified about ten times by a second lens. This magnified view of the projected image was used to evaluate the filter.

The Christiansen filter was positioned in front of the image plane; the distance between the exit plane of the filter and the image plane was adjusted to obtain the desired spatial frequency response.

In color picture telephone operation, a figure for picture bandwidth has not yet been determined. However, at the present time, approximations of 1 MHz for the green, 500kHz for the red, and 300kHz for the blue images may be assumed for a single pickup camera system. By assuming a horizontal line scan time of 100 μs and a raster

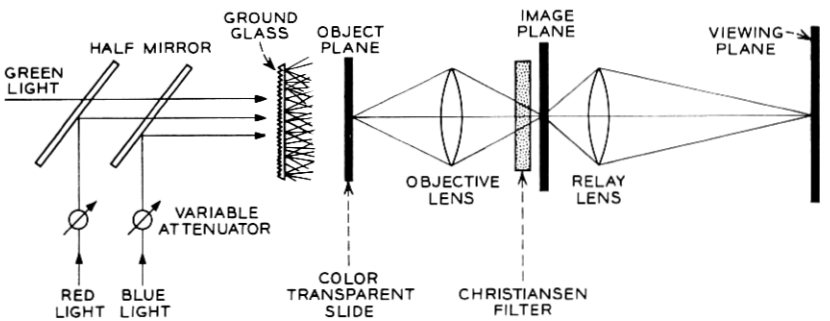

Fig. 10 — Experimental arrangement for evaluation of the Christiansen filter as a resolution controlling device.

size of 12 mm (horizontal), the relationship between the image resolution and required electrical bandwidth is determined.

The spatial frequency response was measured by using a pie-chart test target disk with 30-cycle gratings along the circumference. Since the spatial frequency of the grating varies continuously along the radial direction of the disk, the cutoff frequency of the image can be measured by knowing the point where resolution fails. The image size of the test target was 7.5 mm in diameter.

In order to determine the effectiveness of the filter as a resolution controlling device, an image without the filter was viewed for comparison. In this case the Christiansen filter was replaced by a cell the same size as the filter, filled with only the ethyl salicylate solution. This maintains the same optical path lengths within the imaging system.

5.2 *Image Quality through the Filter*

In order to determine the resolution, each pictoral subject imaged through the system was associated with the corresponding image of the resolution test pattern. This was done by replacing the object slide with the test target object when photographing the system output. The resolutions were determined simply by observing the images of the test pattern resolution chart. The spatial frequency of the test image was 1.27 cycles per mm at the outer edge of the circular pattern. This spatial frequency corresponded to 153 kHz by assuming 100 microseconds for the line scan time and 12 mm for the raster size of the camera tube.

Figure 11a is a photograph of the image formed by incandescent (white) light without the Christiansen filter; Figure 11b is the corresponding photograph of the image of the resolution test pattern. Notice that the same quality images were obtained with separate illumination of each primary color since achromatic lenses were used in the experiment.

Figure 12a is a photograph of the image formed by incandescent (white) light with the Christiansen filter placed 1 mm in front of the image plane. Figure 12b is the corresponding image of the resolution test chart. The distance of 1 mm between the filter and the image plane was chosen to demonstrate the particular case for which the filter will be used in the proposed color camera system. Some of the dark spots in the photographs were caused by the presence of dirt in the filter. Blurring of the image by low-pass filtering is noticeable.

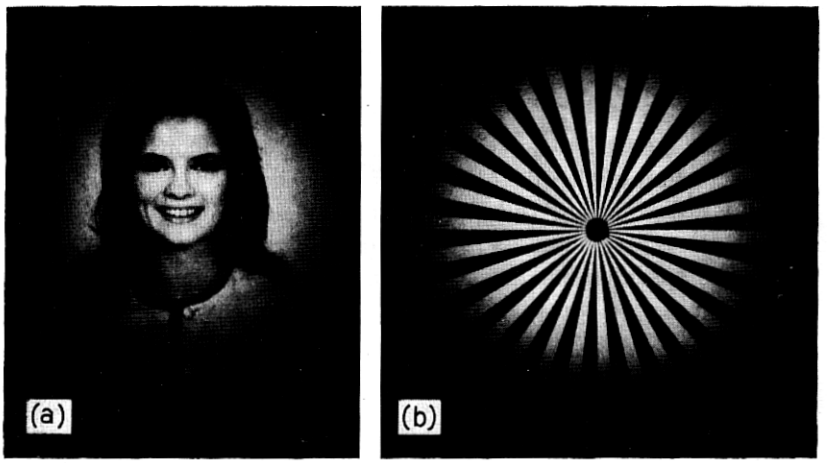

Fig. 11 — (a) Portrait and (b) resolution test chart showing images formed by incandescent (white) light without the Christiansen filter.

This was introduced deliberately by the Christiansen filter and should not be considered as a defect of the optical system. The quality of the image seems acceptable in all other respects.

In order to illustrate to what extent each primary color image in the composite image (Fig. 12) is spatially filtered, three separate

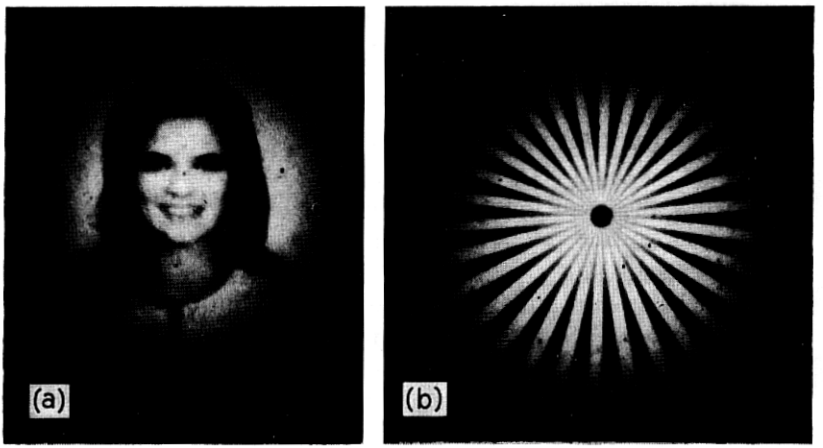

Fig. 12 — (a) Portrait and (b) resolution test chart showing images formed by incandescent (white) light with the Christiansen filter inserted in the optical system.

photographs were taken with each primary color by blocking the other two color sources. Figures 13a and b show photographs of the images formed with green primary light only. The image would be as sharp as that in Fig. 11 if the filter was completely transparent at green. However, the spectral bandwidth of the NTSC green primary color is wider than the matched bandwidth of the filter in green, so that the quality of Fig. 13 is not quite that of Fig. 11. This illustrates that it is advantageous to limit that bandwidth of the green image so that it does not extend beyond the required minimum value.

Figures 14a and b show the images formed with red primary light only. Blurring of the image caused by low-pass spatial filtering by the Christiansen filter is noticeable. The cutoff frequency of the image, determined from Fig. 14b, is about 4 cycles per mm (the resolution falls about one-third of the radius of the pattern) corresponding to a 500 kHz electrical signal.

Similarly, Figs. 15a and b show photographs of the images formed with blue primary light. Blurring of the image is much more noticeable than that of Fig. 14, as expected from characteristics of the Christiansen filter. The cutoff frequency of the image is about 2.5 cycles per mm (the resolution falls about half of the radius of the pattern) corresponding to a 300 kHz electrical signal.

It should be emphasized that although the blurring of the red and blue images is very noticeable when they are viewed alone (as in Figs. 14 and 15), the composite image of all three primaries is of much better quality. This indicates that a significant amount of the detail in the composite image is provided by the green component.[18]

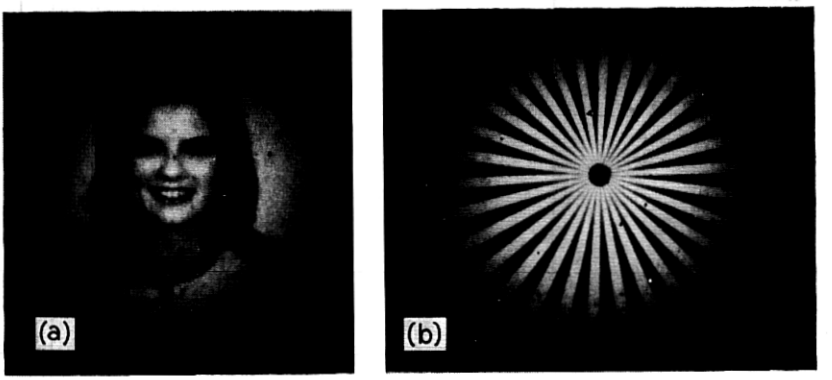

Fig. 13 — Images formed by green primary component color with the filter inserted in the optical system.

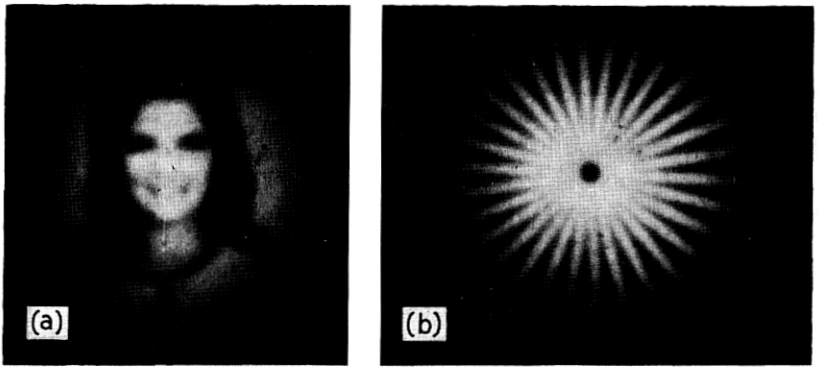

Fig. 14 — Images formed by red primary component color with the filter inserted in the optical system.

In order to illustrate the subjective quality of a composite color image transmitted through this system, Figs. 11a and 12a are printed in color as Figs. 16 and 17, respectively. These photographs were taken on Ektacolor L film.

Much work remains to be done to determine precisely what resolution values should be used, but such a study is beyond the scope of this paper. The point we are trying to make is that we can control the resolution of the three primary color component images and that there is no appreciable degradation beyond that deliberately introduced in the form of spatial bandwidth reduction. Although this system does not have a sharp cutoff characteristic, that is, it does not have a rectan-

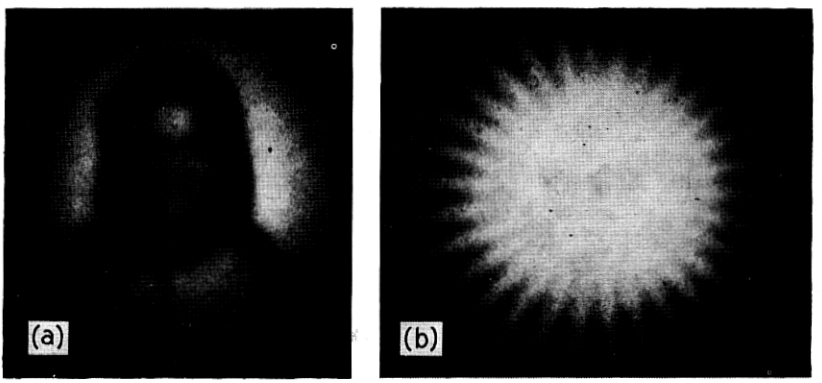

Fig. 15 — Images formed by blue primary component color with the filter inserted in the optical system.

gular passband [see equation (16)], it can nevertheless reduce the image detail of a selected color component by any desired amount, while still permitting coarser image structure to remain.

VI. CONCLUSIONS

Formulas for the modulation transfer function of the Christiansen filter have been derived. The filter thickness, particle size, position of the filter from the image plane, and difference between the particle and liquid indices of refraction have all been shown to control the cutoff frequency but not the shape of the modulation transfer function. The modulation transfer functions as measured with essentially monochromatic sources were in quantitative agreement with those predicted from theory.

The proposed use of the Christiansen filter to reduce the red and blue color detail in a composite image is illustrated using the true "wide band" primary colors. Subjective evaluation of the composite image shows that there is no appreciable degradation beyond that deliberately introduced in the form of spatial bandwidth reduction. The result confirms the applicability of the filter in color picture telephone-like schemes as a means of independently controlling the spatial resolution of the component color images.

VII. ACKNOWLEDGMENTS

The author is grateful to L. H. Enloe for suggesting the problem as well as for his informative advice, and to A. B. Larsen, H. Kogelnik, and Y. S. Yeh for helpful discussions. The use of Mr. F. R. Ashley's lens test apparatus is gratefully acknowledged.

APPENDIX

Random Phase Variation in the Christiansen Filter

When a plane wave is normally incident on the entrance plane of the Christiansen filter, the wave emerges from the filter with the phase varying across its wave front but with no appreciable change in amplitude. The particle size is on the order of hundreds of a wavelength; the difference in refractive index between the particles and liquid is a few parts per thousand. Therefore, the distribution of phase over the emerging wave-front can be described approximately in terms of the distribution of the path length of each ray through the particles.

Since the particles are close-packed, it is assumed that the average

number of particles traversed by a ray as it crosses the filter is uniform. The particles are considered to be spherical with constant radii. The statistical fluctuation in the phase across the exit plane of the filter is caused by the ray passing through different parts of the particles.

Assume the ratio of particle volume to total volume is C and the cross-sectional area of the filter is S. The average number of particles intersected by a single ray which passes through a filter of the thickness L can then be calculated as

$$N = \left(\frac{CSL}{\frac{4}{3}\pi a^3}\right)\left(\frac{\pi a^2}{S}\right) = \frac{3}{4}\frac{CL}{a} \tag{18}$$

where a is radius of the particle. The first parenthesis represents the total number of particles in the filter.

If the ray is traveling in the z direction in the Cartesian coordinates system (x, y, z), the ray path length through an individual particle

Fig. 16 — Ektacolor print of Fig. 11a.

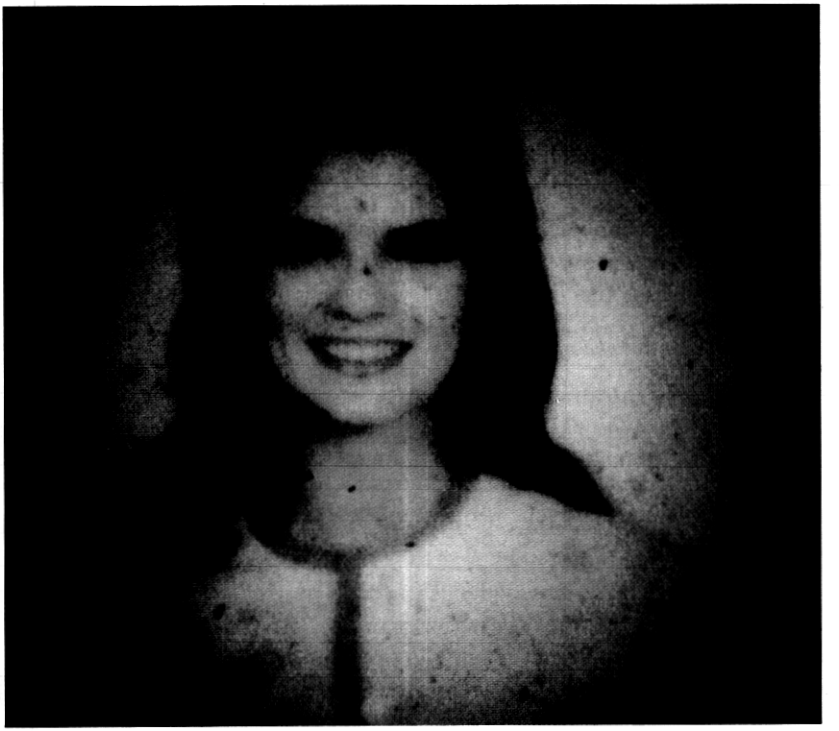

Fig. 17 — Ektacolor print of Fig. 12a.

l will be a function of the lateral displacement of the ray from the particle center in direction x and y. The average path length through a particle is

$$\langle l \rangle_{av} = \int_{-a}^{a} \int_{-(a^2-y^2)^{\frac{1}{2}}}^{(a^2-y^2)^{\frac{1}{2}}} 2(a^2 - x^2 - y^2)^{\frac{1}{2}} P(x, y)\, dx\, dy \qquad (19)$$

where $P(x, y)$ is the probability density function. The lateral displacements in directions x and y are uniformly distributed random variables in the range of the area πa^2. Therefore, $P(x, y)$ is $1/\pi a^2$ and equation (19) becomes

$$\langle l \rangle_{av} = \int_{-a}^{a} \int_{-(a^2-y^2)^{\frac{1}{2}}}^{(a^2-y^2)^{\frac{1}{2}}} 2(a^2 - x^2 - y^2)^{\frac{1}{2}} \frac{1}{\pi a^2}\, dx\, dy = \tfrac{4}{3}a. \qquad (20)$$

This result differs from that obtained by R. H. Clarke, whose probability density function (equation A4 of Ref. 4) depends upon one of the spatial coordinates.

The second moment of l is

$$\langle l^2 \rangle_{av} = \int_{-a}^{a} \int_{-(a^2-y^2)^{\frac{1}{2}}}^{(a^2-y^2)^{\frac{1}{2}}} 4(a^2 - x^2 - y^2) \frac{1}{\pi a^2} \, dx \, dy = 2a^2. \tag{21}$$

Therefore, the variance of the random variable l is

$$\langle l^2 \rangle_{av} - \langle l \rangle^2_{av} = 2a^2 - (\tfrac{4}{3}a)^2 = \tfrac{2}{9}a^2. \tag{22}$$

If the plane wave $E_o(x, y)$ (traveling in direction z) is normally incident to the entrance plane of the filter, the field distribution at the exit plane of the filter can be expressed by the equation

$$E(x, y) = E_o(x, y) \exp \{j\Phi(x, y)\} \tag{23}$$

where $\Phi(x, y)$ is a random phase function.

The phase of the rays at the exit plane of the filter with reference to the average phase across the plane can be written as

$$\Phi = \sum_{m=1}^{N} k \, \Delta n(l_m - \langle l_m \rangle_{av}) \tag{24}$$

where $k = 2\pi/\lambda$ (λ is a wavelength in free space) and Δn is the difference in refractive index between particles and liquid. The process corresponding to each m is an independent random variable so that the summation according to the central limit theorem should be gaussian. This gives

$$P(\Phi) = \frac{1}{(2\pi)^{\frac{1}{2}}\Phi_o} \exp(-\Phi^2/2\Phi_o^2). \tag{25}$$

Thus, the variance of the phase at the exit plane is

$$\Phi_o^2 = \left\langle \left[\sum_{m=1}^{N} k \, \Delta n(l_m - \langle l_m \rangle_{av}) \right]^2 \right\rangle_{av} = N(k \, \Delta n)^2 \langle (l - \langle l \rangle_{av})^2 \rangle_{av} + N(N-1)(k \, \Delta n)^2 \langle (l - \langle l \rangle_{av}) \rangle^2_{av} . \tag{26}$$

Noting that the second term is zero and using equations (18) and (22), equation (26) becomes

$$\Phi_o^2 = N(k \, \Delta n)^2 \tfrac{2}{9}a^2 = \frac{6.58CLa \, \Delta n^2}{\lambda^2}. \tag{27}$$

REFERENCES

1. Christiansen, C., "Untersuchungen uber die optischen Eigenschaften von feinvertheilten Korpern," Annalen der Physik und Chemie, *23* No. 10 (1884), pp. 298–306.

2. McAlister, E. D., "The Christiansen Light Filter: Its Advantages and Limitations," Smithsonian Miscellaneous Collections, *93,* No. 7 (April 1935), pp. 1–11.
3. Raman, C. V., "The Theory of the Christiansen Experiment," Proc. India Acad. Sci., *A29,* (1943), pp. 381–390.
4. Clarke, R. H., "A Theory for the Christiansen Filter," Appl. Opt., *7,* No. 5 (May 1968), pp. 861–868.
5. Kell, R. D., "Color Television Camera," U. S. Patent No. 2,733,291, applied for July 29, 1952 issued January 31, 1956.
6. Takagi, T., and Nagahara, S., "Single-Pickup-Tube Color Camera System," Japan Elec. Eng., No. 11, (1967), pp. 41–44.
7. Ratcliffe, J. A., "Some Aspects of Diffraction Theory and Their Application to the Ionosphere," Rep. Progress Phys., *19,* (1956), pp. 188–267.
8. Brown, E. B., *Modern Optics,* New York: Reinhold Publishing, 1965, p. 484.
9. Born, M., and Wolf, E., *Principles of Optics,* New York: Pergamon Press, 1965, 3rd ed., p. 370.
10. Leith, E. N., and Palermo, C. J., "Introduction to Optical Data Processing," University of Michigan Eng. Summer Conf., May 24–June 4, 1965, pp. 2–12 to 2–28.
11. Van der Lugt, A., "Operational Notation for the Analysis and Synthesis of Optical Data-Processing Systems," Proc. IEEE, *54,* No. 8 (August 1966), pp. 1055–1063.
12. O'Neill, E. L., *Introduction to Statistical Optics,* Reading, Massachusetts: Addison-Wesley, 1963, p. 100.
13. Rowe, H. E., *Signals and Noise in Communication Systems,* New York: Van Nostrand, 1965, pp. 125–135.
14. Tatarski, V. I., *Wave Propagation in a Turbulent Medium,* New York: McGraw-Hill, 1961), p. 6.
15. Booker, H. G., and Gordon, W. E., "A Theory of Radio Scattering in the Troposphere," Proc. Inst. Radio Engineers, *38,* No. 4 (April 1950), p. 401.
16. Pekeris, C. L., "Note on the Scattering of Radiation in an Inhomogeneous Medium," Phys. Rev., *71,* No. 4 (February 1947), p. 268.
17. Herriott, D. R., "Recording Electronic Lens Bench," J. Opt. Soc. Amer., *48,* No. 12 (December 1958), pp. 968–971.
18. Baldwin, M. W., Jr., "Subjective Sharpness of Additive Color Picture," Proc. IRE, *39,* No. 10 (October 1951), pp. 1173–1176.